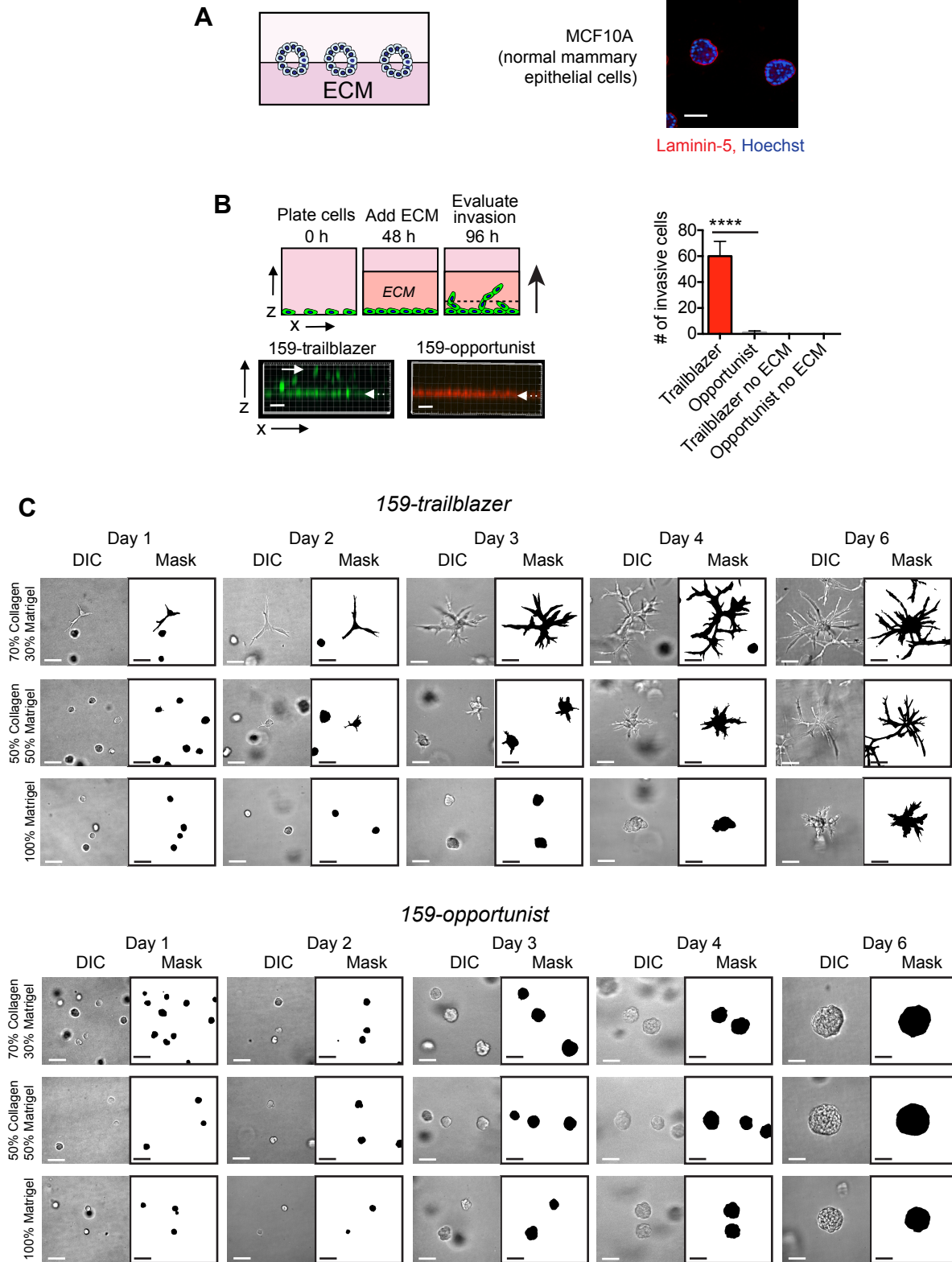
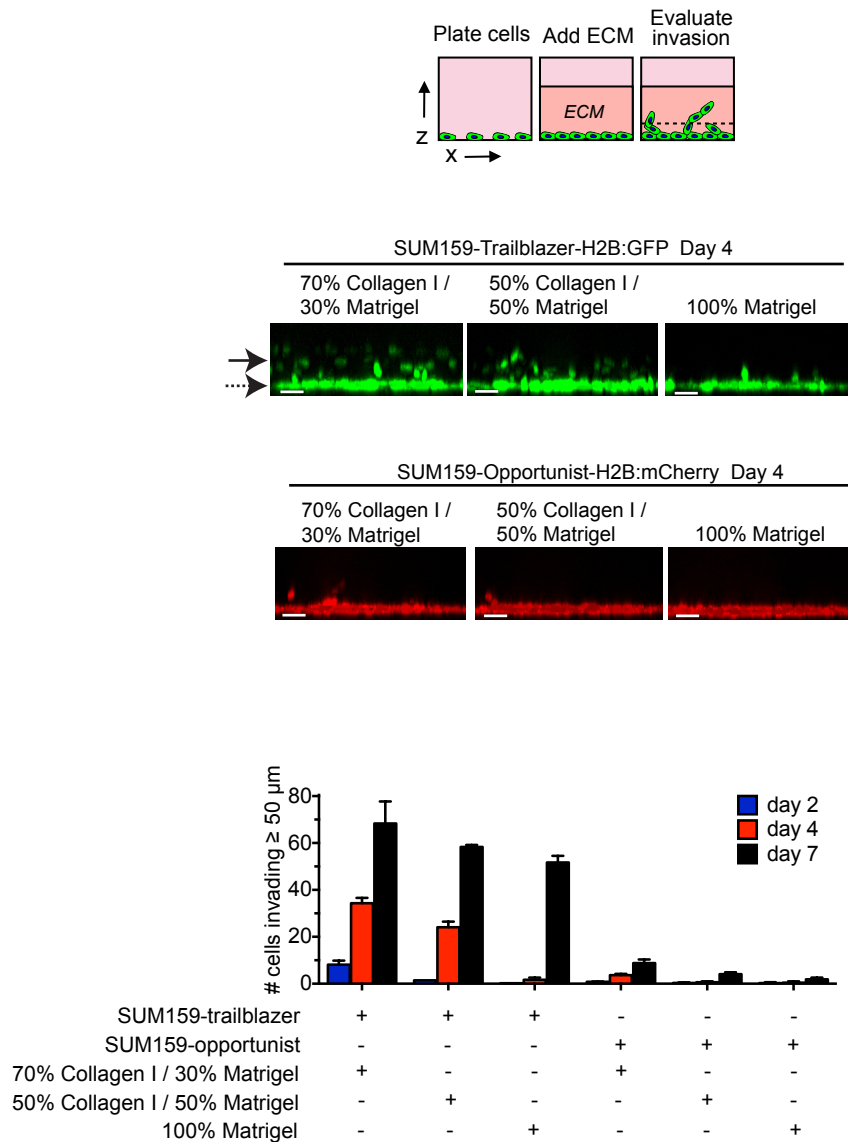


Supplemental Figure 1 (Westcott et. al.)



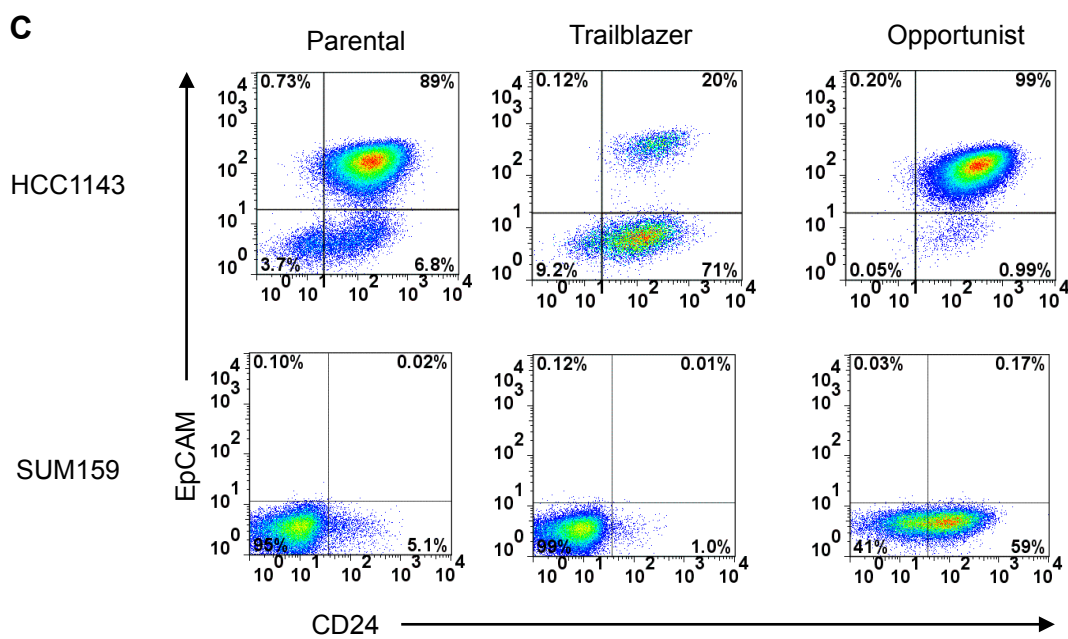
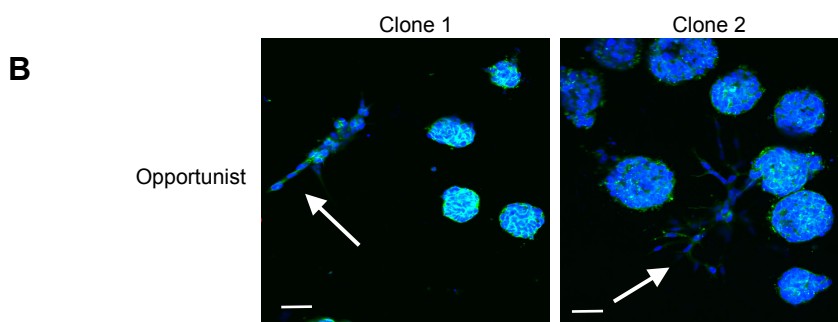
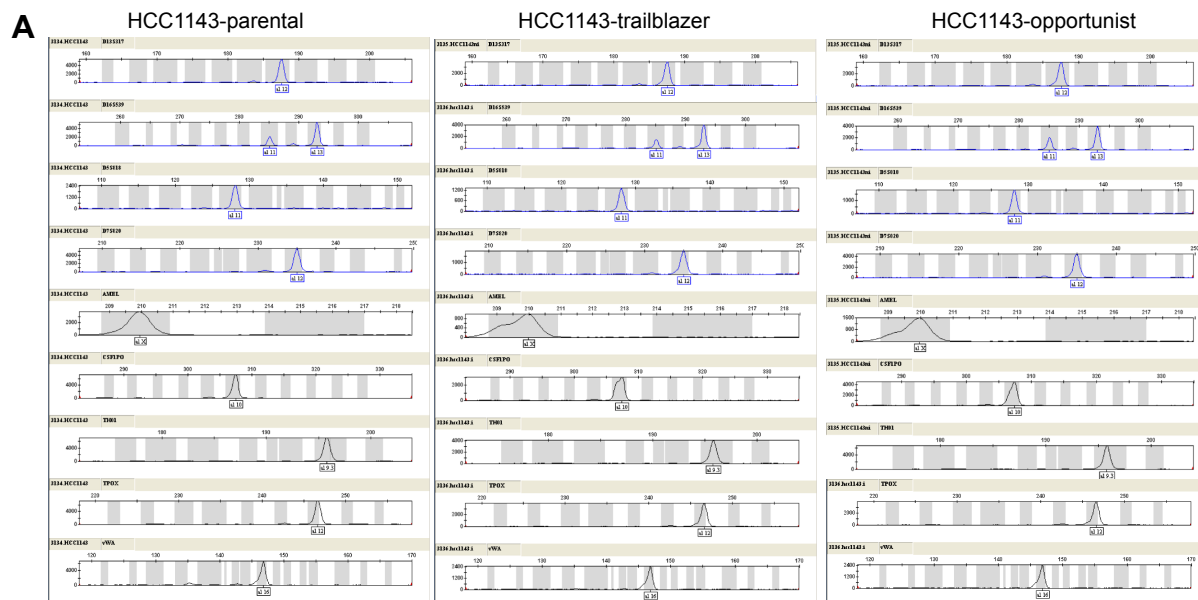
Supplemental Figure 1. (A) Representative image of MCF10A non-transformed mammary epithelial cells were grown in organotypic culture for 10 days and stained as indicated (n=3). Scale bars, 50 μ m. (B) Representative x-z views of SUM159-trailblazer and SUM159-opportunist cell invasion into the ECM. Dotted white arrow indicate the cell monolayer. Solid white arrow indicates invasive cells. Scale bars, 50 μ m. Graph shows the number of cells invading $\geq 50 \mu$ m (mean +SD, n=3) ****p< 0.0001, unpaired Student's t-test. (C) SUM159-trailblazer and SUM159-opportunist cells were grown in organotypic culture on the indicated ratios of Collagen I and Matrigel. Images were acquired on Days 1, 2, 3, 4 and 6. Representative images and masks of the outline of the spheroids are shown (n= 3). Scale bars, 50 μ m.

Supplemental Figure 2 (Westcott et. al.)



Supplemental Figure 2. Representative x-z views of SUM159-trailblazer and SUM159-opportunist cell invasion into ECM consisting of the indicated ratios of Collagen I and Matrigel. Dashed arrow indicates the cell monolayer. Solid arrow indicates invasive cells. Scale bars, 50 μm . Graph shows the number of cells invading $\geq 50 \mu\text{m}$ at the indicated number of days after addition of ECM (mean \pm SD, n=3).

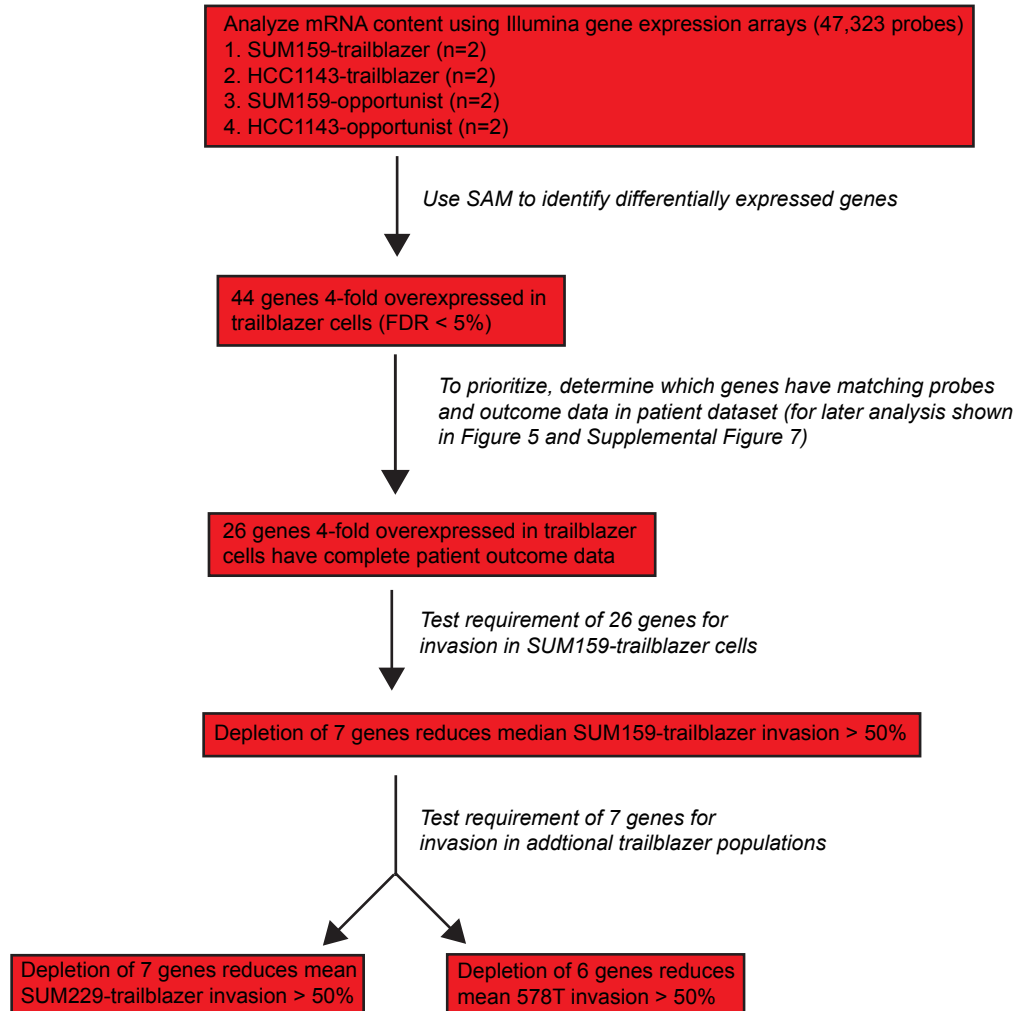
Supplemental Figure 3 (Westcott et. al.)



Supplemental Figure 3. (A) Powerplex fingerprinting of the HCC1143-parental, trailblazer and opportunist cells. (B) Representative images of spheroids from 2 distinct daughter clonal cell lines initiated by single opportunist cells (n=3). Solid arrows indicate invasive spheroids. Scale bars, 50 μ m. (C) Representative FACS analysis of EpCAM and CD24 expression in the indicated cells.

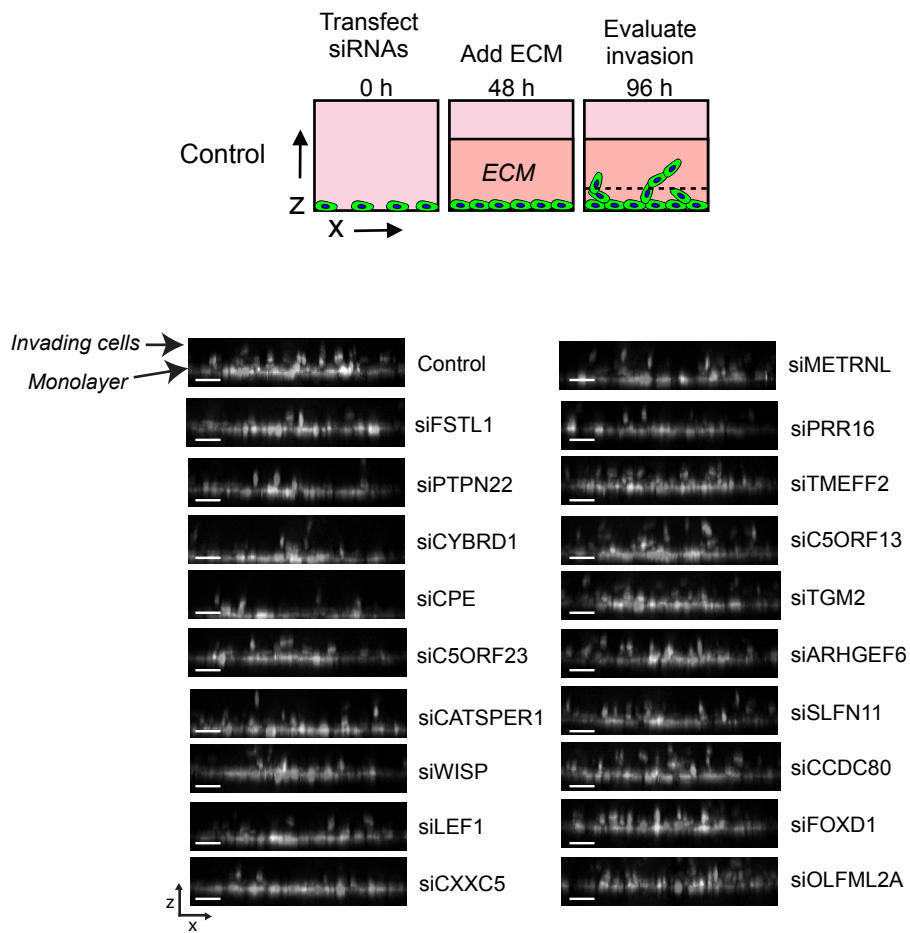
Supplemental Figure 4 (Westcott et. al.)

Workflow to determine if genes highly expressed in trailblazer cells contribute to invasion



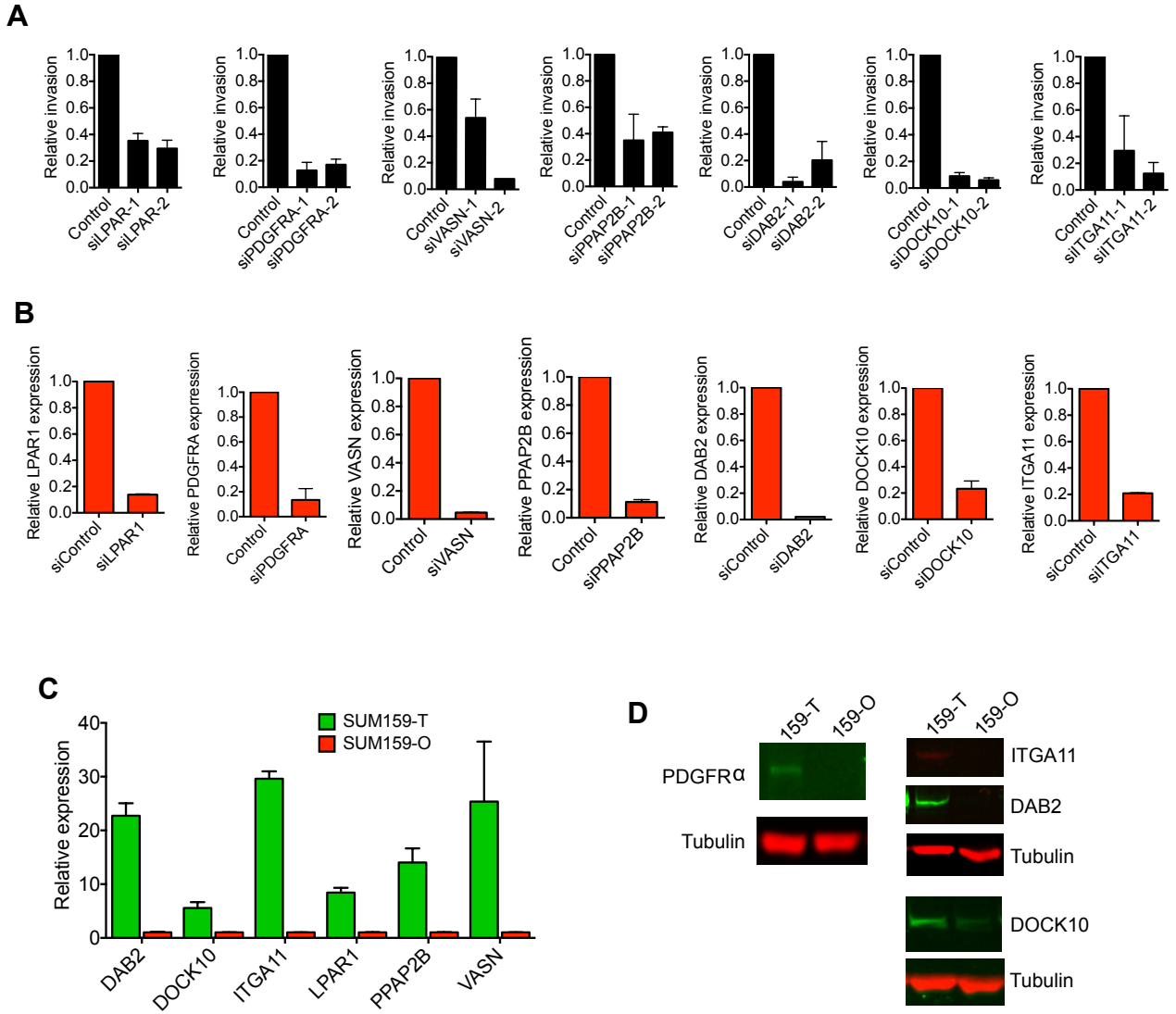
Supplemental Figure 4. Workflow for determining if genes highly expressed in trailblazer cells are required for collective invasion.

Supplemental Figure 5 (Westcott et. al.)



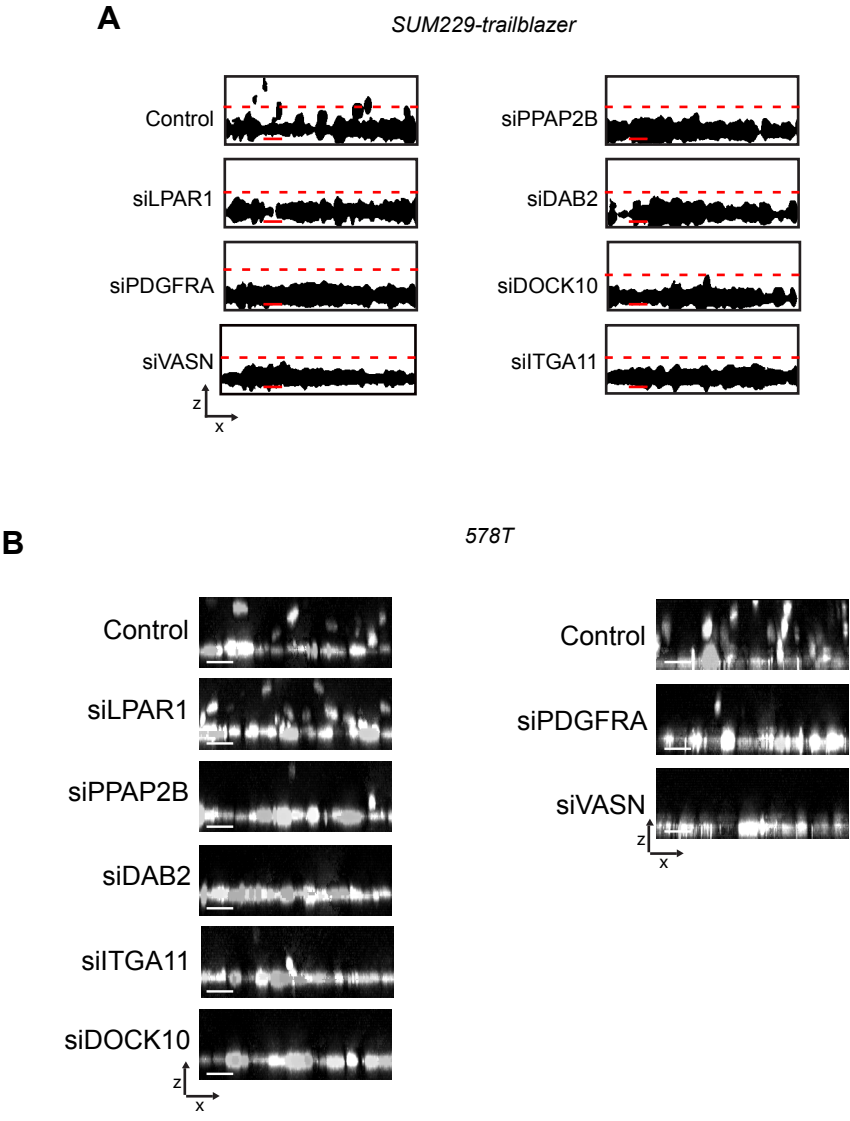
Supplemental Figure 5. Representative images are x-z views of SUM159-trailblazer invasion into ECM after transfection with the indicated siRNAs (n=3). Fluorescent nuclei are shown. Scale bar, 50 μm. These images correspond to the quantification shown in Figure 4B.

Supplemental Figure 6 (Westcott et. al.)



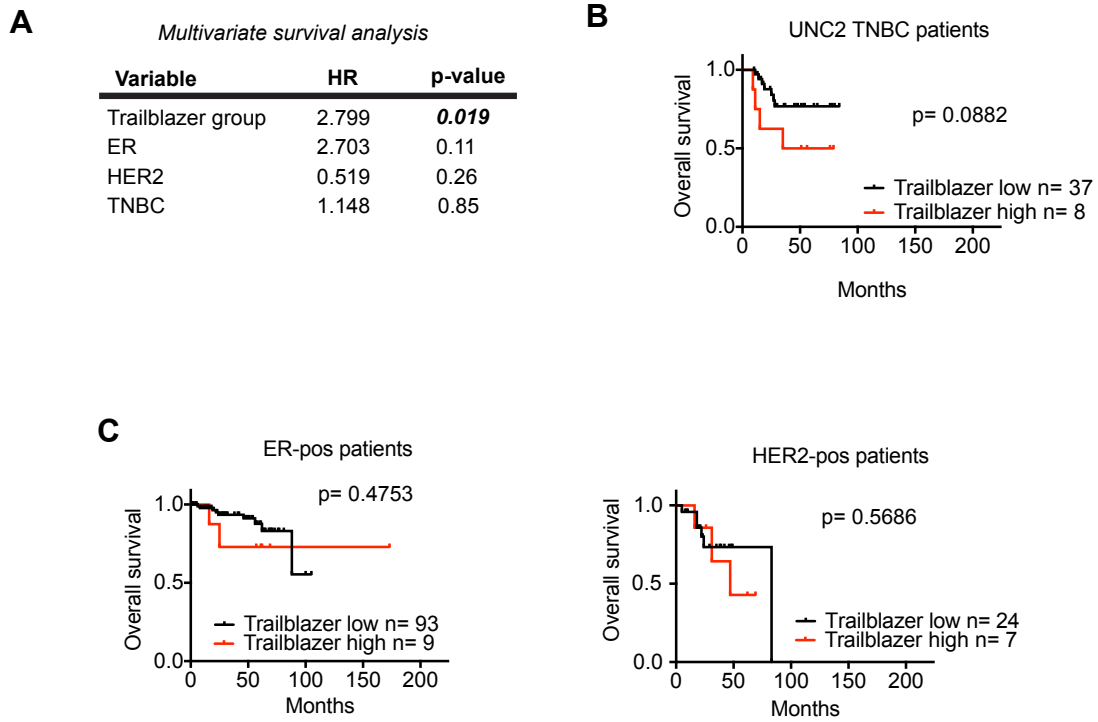
Supplemental Figure 6. (A) Graphs show the relative invasion of SUM159-trailblazer cells transfected with 2 distinct siRNAs targeting the indicated genes (mean + range, n=2, performed in duplicate for 4 total wells). (B) Graphs show the relative normalized expression of the indicated genes after transfection with siRNAs for 72 h as determined by q-PCR (mean+SD of triplicate values from a representative experiment, n=2). (C) Graph shows the relative expression of the indicated genes in the SUM159-trailblazer and SUM159-opportunist subpopulations as determined by q-PCR (mean+SD of triplicate values from 2 experiments). (D) Representative immunoblots show the expression of PDGFRA, ITGA11, DAB2 and DOCK10 in the SUM159-trailblazer and SUM159-opportunist subpopulations (n=3). Tubulin expression serves as a loading control. T= trailblazer, O= opportunist.

Supplemental Figure 7 (Westcott et. al.)



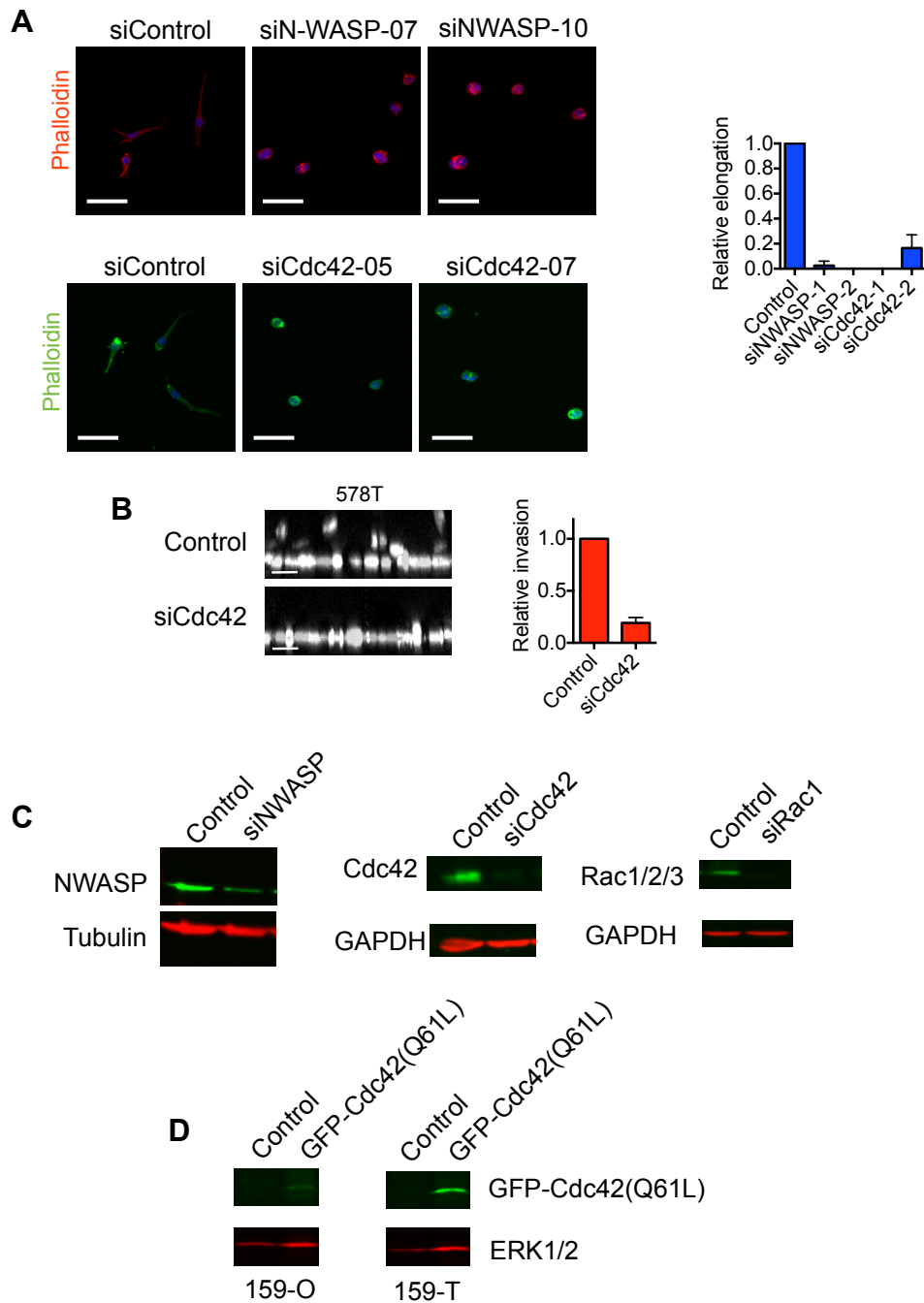
Supplemental Figure 7. (A) Representative x-z views of SUM229-trailblazer invasion into the ECM after transfection with the indicated siRNAs. Image masks of fluorescent nuclei are shown. Scale bar, 50 μ m. **(B)** Representative x-z views of 578T invasion into the ECM after transfection with the indicated siRNAs (n=3). Fluorescent nuclei are shown. Scale bar, 50 μ m. Fluorescent nuclei are shown. Images are from 2 different experiment groups, (Control, siLPAR1, siPPAP2B, siDAB2, siITGA11, siDOCK10) and (Control, siPDGFRA, siVASN). Scale bar, 50 μ m. The images correspond to the quantification shown in Figure 4E.

Supplemental Figure 8 (Westcott et. al.)



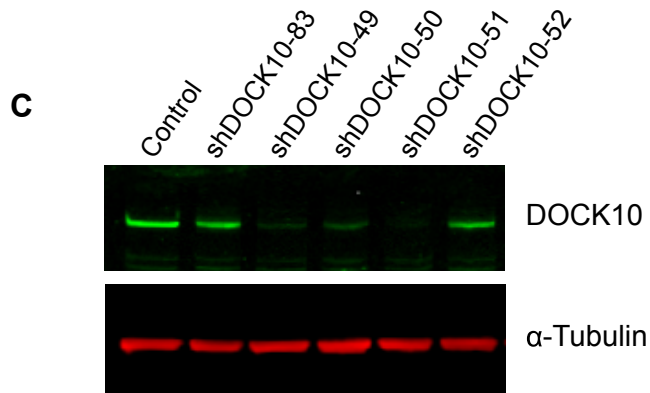
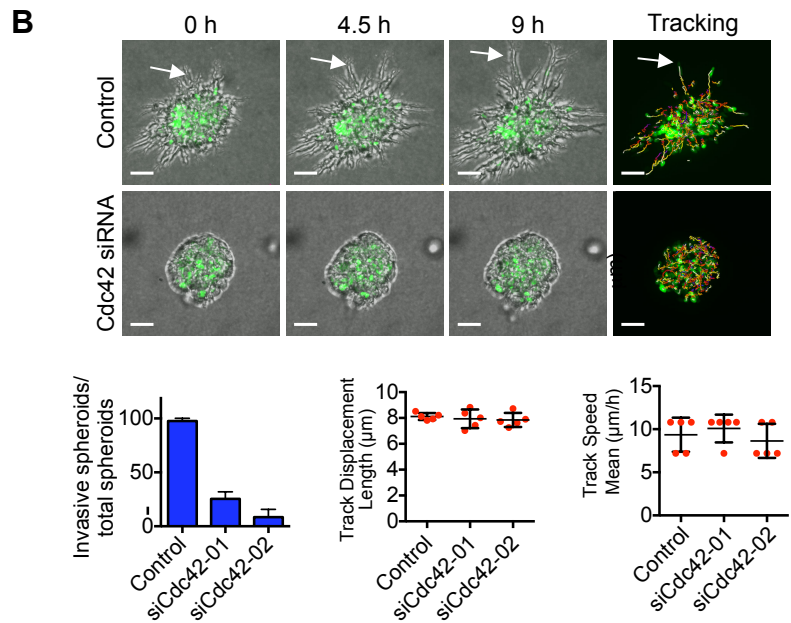
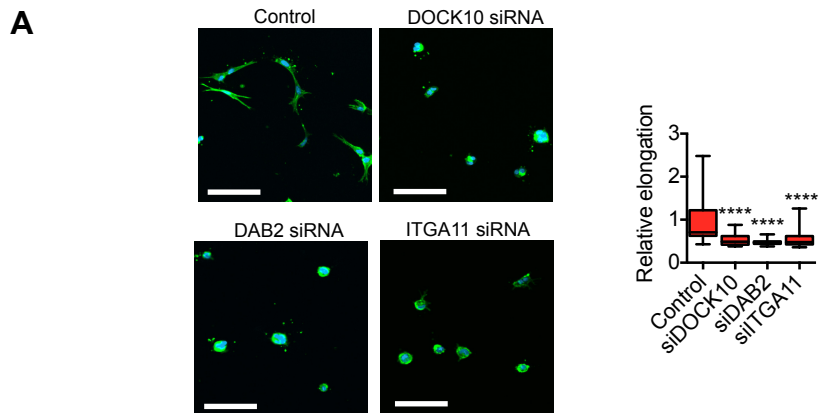
Supplemental Figure 8. (A) Cox regression model which includes Trailblazer group, ER, HER2, and TNBC classification as variables. (B) Kaplan-Meier survival curves for from second independent set of TNBC patients classified into “Trailblazer high” and Trailblazer low” groups. Survival differences were compared using the log-rank (Mantel-Cox) test. (C) Kaplan-Meier survival curves for ER-positive (ER-pos) and HER2-positive (HER2-pos) patients classified into “Trailblazer high” and Trailblazer low” groups in Figure 5. Survival differences were compared using the log-rank (Mantel-Cox) test.

Supplemental Figure 9 (Westcott et. al.)



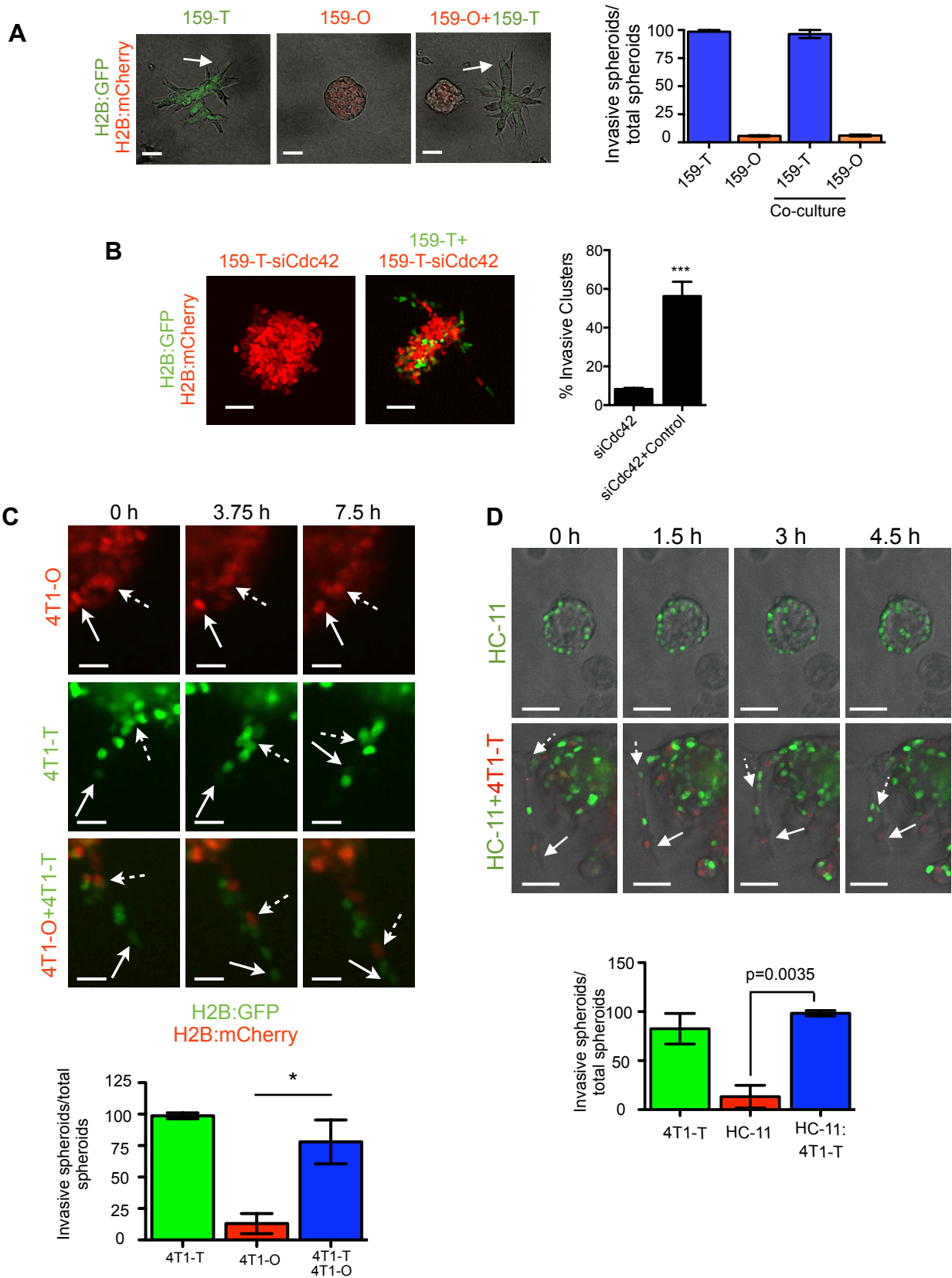
Supplemental Figure 9. (A) SUM159-trailblazer cells transfected with the indicated siRNAs were plated onto a layer of ECM for 24 h and stained. Scale bar, 50 μ m. Representative images are shown. Bar graph shows the relative length of LCPs as determined by length/width of the cells (mean+ range, 50 cells/condition, n=2). (B) Representative x-z views of SUM159-trailblazer invasion into the ECM after transfection with Control or Cdc42 siRNAs. Fluorescent nuclei are shown. n=3. Scale bar, 50 μ m. Graph shows the relative invasion of 578T cells transfected with the control or Cdc42 siRNAs (mean+SD, n=3). (C) Representative immunoblots of SUM159-trailblazer cells 48 h after transfection with the indicated siRNAs (n=3). (D) Representative immunoblots of SUM159-trailblazer and SUM159-opportunist cells stably expressing a control vector or GFP-Cdc42(Q61L) (n=3). Lysates were immunostained with anti-Cdc42 (top) and anti-ERK1/2 antibodies (bottom).

Supplemental Figure 10 (Westcott et. al.)



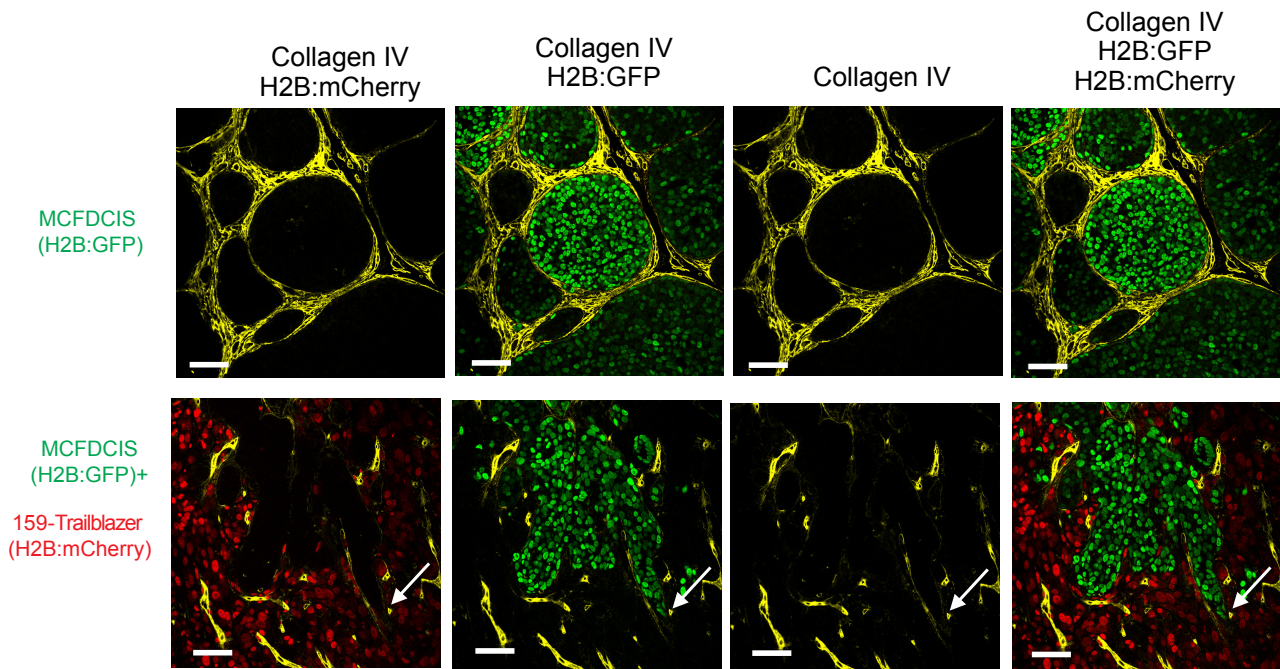
Supplemental Figure 10. (A) 578T cells transfected with the indicated siRNAs were plated onto a layer of ECM for 24 h and stained. Scale bar, 50 μ m. Representative images are shown. Graph shows the relative length of LCPs as determined by length/width of the cells (mean \pm SD, 20 cells/condition, n=3). ****p< 0.0001, unpaired Student's t-test. (B) Representative time lapse bright field images and tracking of SUM159-trailblazer cells transfected with the 2 different Cdc42 targeting siRNAs and clustered into spheroids. Solid arrows identify invasive projections. Tracking of cell movement in the representative spheroids is shown in the right-hand panels. Scale bar, 50 μ m. Graphs shows the percent of invasive spheroids (mean \pm SD, n=3) and the speed and displacement of cells within the spheroids (mean \pm SD, of 5 spheroids/condition in a representative experiment, n=3). (C) Representative immunoblot of SUM159 trailblazer cells stably expressing control shRNA or shRNAs targeting DOCK10 (n=3). SUM159-trailblazer cells expressing the shDOCK10-51 were used for the xenograft experiments shown in Figure 7.

Supplemental Figure 11 (Westcott et. al.)



Supplemental Figure 11. (A) SUM159-opportunist and SUM159-trailblazer subpopulations were plated alone or together at a 50:50 ratio in organotypic culture. Under these conditions, the spheroids are clonal. Representative images are shown. Solid arrows identify invasive projections. Graph shows the percent of invasive spheroids (mean± range, 50 spheroids/condition ind duplicate, n=2). Scale bar, 50 µm. **(B)** SUM159-trailblazer-H2B:mCherry cells were transfected with the Cdc42 siRNAs for 24 h before clustering alone or with control SUM159-trailblazer-H2B:GFP cells in spheroids at 4:1 ratio. Spheroid clusters grown for 48 h in organotypic culture are shown. Representative images are shown. Solid arrows indicate invasive projections. Scale bar, 50 µm. Graph show the percent of invasive spheroids (mean +SD, 50 spheroids/condition, n=3). ***p <.001, unpaired Student's t-test. **(C)** Representative time-lapse images of spheroids composed of 100% 4T1-trailblazer, 100% 4T1-opportunist, or 20% 4T1-trailblazer/80% 4T1-opportunist cells. Solid arrows indicate cells leading invasion. Dotted arrows indicate cells following into an existing invasive projection. Bar, 25 µm. Graph shows the percent of invasive spheroids (mean ± SEM of 30 spheroids/condition, n= 3). *p <0.05, unpaired Student's t-test. T= trailblazer, O= opportunist. **(D)** Representative time-lapse images of spheroids composed of 100% 4T1-trailblazer, 100% HC-11 or 10% 4T1-trailblazer/90% HC-11 cells. Solid arrows indicate areas of invasion and dotted arrows indicate cells following into an existing invasive projection. Scale bar, 25 µm. Graph shows the percent of invasive spheroids (mean ± SD of 10 spheroids/condition, n= 3). **p <0.01 unpaired Student's t-test.

Supplemental Figure 12 (Westcott et. al.)



Supplemental Figure 12. Representative immunostaining of primary tumors composed of MCFDCIS cells alone or a mix of MCFDCIS and SUM159-traiblazer cells (1:1 ratio) with the indicated antibodies. Solid arrows indicate representative areas of invasion (MCFDCIS n= 10 mice, MCFDCIS + SUM159-traiblazer, n= 10 mice).

Supplemental Legends

Supplemental Table 1. Genes with ≥ 4 -fold increased expression in the both the HCC1143-trailblazer and SUM159-trailblazer cells compared to the HCC1143-opportunist and SUM159-opportunist cells with a F.D.R. of 0.05.

Supplemental Table 2. List of siRNA sequences used.

Supplemental Video 1. Live imaging of an invasive SUM159 spheroid (H2B:GFP, green, nuclei) showing cell motility in organotypic culture. Fluorescent and bright field images were acquired at 15 min intervals over a span of 7.5 h. This Video corresponds with the tracking of cell movement in the trailblazer SUM159 spheroid shown in Figure 1C.

Supplemental Video 2. Live imaging of a noninvasive SUM159 spheroid (H2B:mCherry, red, nuclei) showing cell motility in organotypic culture. Fluorescent and bright field images were acquired at 15 min intervals over a span of 7.5 h. This Video corresponds with the tracking of cell movement in the opportunist SUM159 spheroid shown in Figure 1C.

Supplemental Video 3. Live imaging of a SUM159-trailblazer clustered spheroid (H2B:GFP, green, nuclei) showing cell motility. Fluorescent and bright field images were acquired at 30 min intervals over a span of 13 h. This is the time lapse imaging of the SUM159-trailblazer spheroid shown in Figure 8C.

Supplemental Video 4. Live imaging of a SUM159-opportunist clustered spheroid (H2B:mCherry, red, nuclei) showing cell motility. Fluorescent and bright field images were

acquired at 30 min intervals over a span of 13 h. This is the time lapse imaging of a SUM159-opportunist spheroid shown in Figure 8C.

Supplemental Video 5. Live-imaging of a heterogenous spheroid containing SUM159-trailblazer cells (H2B:GFP, green, nuclei) clustered with SUM159-opportunist cells (H2B:mCherry, red, nuclei). Fluorescent and bright field images were acquired at 30 min intervals over a span of 13 h. This is the time lapse imaging of a heterogenous SUM159-trailblazer/SUM159-opportunist spheroid shown in Figure 8C.

Supplemental Video 6. Fluorescent imaging of a heterogenous spheroid containing SUM159-trailblazer cells (H2B:GFP, green, nuclei) clustered with SUM159-opportunist cells (H2B:mCherry, red, nuclei). This is the fluorescent signal showing just the cell nuclei from the time lapse imaging of the heterogenous SUM159-trailblazer/SUM159-opportunist spheroid shown in Figure 8C and Supplemental Video 6.

Supplemental Methods

Cell Culture conditions. T47D, HCC1143, HCC1428, HCC1569, HCC1954, 4T1 and HC-11 cells were cultured in a base medium of RPMI (Hyclone), 10% fetal bovine serum (FBS, Hyclone) and 1x penicillin streptomycin solution (Hyclone). HCC1143 medium was supplemented with 5 ng/ml EGF (Sigma), T47D medium was supplemented with 10 µg/ml insulin (Sigma) and HC-11 medium was supplemented with 10 ng/ml EGF and 5 µg/ml insulin. SUM159 cells were cultured in Ham's F-12 medium containing 5% fetal bovine serum (FBS, Hyclone), 1x penicillin streptomycin solution (Hyclone), 5 µg/ml insulin (Sigma Aldrich), and 1mg/ml hydrocortisone (Sigma-Aldrich). SUM149 were grown in 5% FBS mammary epithelial growth medium (MEGM, Lonza).

Quantification of spheroid invasion. For assays in which spheroids developed from a single cells, a spheroid was classified as invasive if 3 or more cells invaded away from a primary spheroid containing 10 or more cells. For assays analyzing spheroid clusters generated in hanging drops before culturing, only spheroids composed of at least 50 cells and heterogeneous clusters were analyzed. For heterogeneous clusters, only spheroids containing that contained 10% or more trailblazer cells were quantified. The heterogenous spheroid projection to be classified as "invasive", it had to contain at least one opportunist cell in an invasive projection. The number of spheroids counted per condition and replicates are indicated in the Figure Legends.

Quantification of LCPs. The dimensions of at least 10 cells per duplicate well from 3 separate experiments were measured using ImageJ software. Briefly, 5X images of phalloidin-stained cultures were thresholded for brightness to trace cell edges, and then the 'Analyze...' function of ImageJ was used to obtain length and width measurements. Relative elongation was determined by calculating the ratio of length over width (L/W) and then normalizing these

values to control L/W ratios. The L/W ratio reflects that relative elongation of the cell, which is directly influenced by the formation of LCPs.

Vertical invasion of tumor cells into ECM. 10,000 cells (consisting of H2B:GFP- and H2B:mCherry-labeled cells mixed at a 1:4 ratio) were reverse transfected in duplicate in a 96-well plate with 50 nM OnTargetplus siRNAs using RNAiMax transfection reagent (Invitrogen). The use of 2 colors allows for a more accurate quantification of the total cell number using image analysis. After 48 hrs, media was replaced with 50 μ l Matrigel/Collagen matrix (5 mg/ml Matrigel and 2.1 mg/ml Collagen I, unless indicated otherwise), followed by growth media, and incubated at 37°C. Forty-eight h after ECM addition, cells were imaged with a 20X objective on a Perkin Elmer Ultraview spinning disk confocal microscope equipped with a CCD camera (Hamamatsu). Thirty-one z -slices at 5- μ m intervals over a total span of 150 μ m were acquired for 10 x,y positions per well that were randomly selected by Volocity software (Perkin Elmer). At least 2 wells (20 x,y positions total) were imaged per condition in each experiment. ImageJ software (NIH) was used to process images and quantify invasion. Relative invasion was calculated by counting the total number of H2B:mCherry-labeled cells that had migrated 50 μ m or more above the monolayer. To correct for possible differences in proliferation rates, the total relative cell number for each well was determined by counting the number of H2B:GFP-labeled cells in the monolayer. The number of invading cells was then divided by the number of monolayer cells to determine the normalized invasion for each well. To determine the relative invasion for each experiment, the normalized invasion value for each condition was divided by the normalized invasion for the control wells transfected with an siRNA pool that does not target human genes.

Real-time imaging of organotypic cultures. Imaging was performed using a Perkin Elmer Ultraview ERS spinning disk confocal microscope enclosed in a 37°C chamber supplemented with humidified CO₂ (Solent) and a CCD camera (Orca AG; Hamamatsu).

Images were acquired with a 20x (Zeiss) objective using Volocity software (Perkin Elmer) and analyzed with Imaris software (Bitplane). At least 6 to 10 different x,y coordinates with 6 to 14 z-slices over 60-140 μm span for each condition were imaged in parallel.

Daughter subpopulation isolation. Parental cell lines were plated in organotypic culture for at least 8 days. To isolate the spheroids, 4°C PBS was added to each well to dissolve the Matrigel/Collagen I. Spheroids were then isolated by pipetting into microfuge tubes based on phenotype using a phase contrast microscope. Spheroids with 4 or more projections of at least 3 cells were considered “trailblazer” and spheroids with no cellular projections were considered “opportunist”. Spheroids were then trypsinized into a single cell suspension and replated in organotypic culture and re-isolated. This process was repeated up to 2 additional times before expansion in monolayer culture to establish independent daughter cell lines.

Flow cytometry and antibodies. For each sample, 5×10^5 cells were washed and resuspended in PBS supplemented with 2% FBS. Cells were mixed with antibody diluted in 2% FBS PBS and incubated for 20 min in the dark at 4 °C. Samples were then washed and resuspended in propidium iodide diluted in 2% FBS/PBS. At least 50,000 events were collected on an LSRII flow cytometer (Becton Dickinson), and analyzed using Flow Jo software (Tree Star Technologies).

Fluorescence activated cell sorting. For each cell line, a total of 20×10^6 cells were stained with fluorescently-conjugated antibodies specific for human EpCAM, as described above. Cells were resuspended at 20×10^6 cells/ml in 2% FBS PBS containing propidium iodide, and then FACS sorted into EpCAM-lo and EpCAM-hi subpopulations. Sorted cells were then replated in growth media and cultured for 5-10 days before being replated in organotypic culture.

Immunoblot analysis and immunofluorescence staining. Cells were lysed in RIPA buffer supplemented with a protease inhibitor cocktail (Calbiochem) as described (Pearson and

Hunter 2007). Equal amounts of protein were separated by SDS-PAGE, transferred to Immobilon-FL polyvinylidene fluoride (PVDF) transfer membrane (Millipore), and immunostained. Immunoblots were visualized using an Odyssey infrared scanner (LI-COR). Organotypic cultures were fixed and immunostained as described (Pearson and Hunter 2007). Images were acquired on Nikon and Zeiss LSM510 confocal microscopes in TIFF format. Images were arranged using Photoshop CS3 (Adobe) and Keynote (Apple). Where indicated, images “masks” were created with Fiji software using maximum intensity projections of each image. For each projection, actin signals were thresholded for brightness and then converted to binary masks.

DOCK10 shRNA virus production and infection. For stable RNAi-mediated knockdown of DOCK10 in SUM159 cells, five DOCK10-specific shRNA clones in the MISSION pLKO.1-puro vector, and one control vector (SHC001) were purchased from Sigma-Aldrich (St. Louis, MO). The shRNA sequence of the DOCK10-51, which was used in our metastasis assays, was:

CCGGCCAGGATTCCAACAAGGTAAACTCGAGTTTACCTTGTTGGAATCCTGGTTTTTG

(TRCN0000122951, MISSION TRC1 shRNA Target Set; Sigma). Lentiviral particles were generated by co-transfecting HEK293 cells with DOCK10 shRNA constructs, plus pMDL-, RSV-REV-, and VSVG-expressing packaging plasmids. Transfections were carried out with Lipofectamine 2000 transfection reagent, in accordance with the manufacturer’s protocols (Invitrogen, Carlsbad, CA). SUM159-trailblazer cells expressing GFP and luciferase were infected with shDOCK10 or control lentiviruses and then reinfected after 24 hours. Stable cell lines were selected and maintained with 5µg/ml puromycin.

Xenograft experiments. Age-matched female NOD/SCID mice were used for all in vivo experiments. When possible, littermates were housed together. NOD/SCID mice were obtained

from The Jackson Laboratory (Bar Harbor, ME), and bred and maintained under specific pathogen-free conditions in a barrier facility at the University of Texas Southwestern Medical Center (Dallas, TX). All experiments were performed in compliance with the relevant laws and institutional guidelines of the University of Texas Southwestern Medical Center. For spontaneous metastasis experiments, 500,000 SUM159-trailblazer cells stably expressing GFP, luciferase, and either shDOCK10-51, or control pLKO.1 constructs were injected into the #4 fat pad of 6-8-week old female NOD/SCID mice. A total of 9 mice were injected per condition. Bioluminescent imaging (BLI) was used to measure primary tumor growth. After 42 days, BLI measurements of primary tumors were acquired, after which mice were immediately sacrificed. Both tumors and lungs were excised, and lung metastases were quantified ex vivo with BLI and a fluorescent dissecting microscope by counting the number of clusters of at least 1 GFP expressing cell in at least 3 fields of view per lung. For mixed-cell xenografts, 6-8-week old female NOD/SCID mice were injected in the #4 fat pad with 50,000 MCFDCIS cells expressing H2B:GFP and/or 50,000 SUM159-Trailblazer cells expressing H2B:mCherry. A total of 5-10 mice were injected per condition in 2 separate experiments. After 25 days, mice were sacrificed and primary tumors were excised. Tumors were then formalin-fixed and paraffin-embedded for further immunohistochemical analysis.

Tumor explants. For tumor explant studies, 500,000 SUM159-trailblazer cells were injected into the #4 fat pad of 6-8 week old female NOD/SCID mice. Three weeks after injection, mice were sacrificed and tumors were excised and minced into approximately 1 mm³ pieces using a scalpel. Minced tumors were digested for 45-60 min, shaking, at 37°C in a mixture of 1mg/ml Collagenase, 2U/μl DNase, 5% FBS in complete mammary epithelial growth medium (MEGM)(Lonza). Digested tumors were pelleted at 80 x g for 1 min and the supernatant was discarded. Tumor organized were then and rinsed 5 times in 10 ml MEGM +5% FBS. Tumor pieces were resuspended in 300 μl ECM (21. mg/ml Collagen I + 3 mg/ml

Matrigel), and plated onto 300 μ l of solidified ECM in a 24-well plate and overlaid with MEGM + 5% FBS. For isolation of primary mouse mammary organoids, 4th and 9th inguinal mammary glands were removed from 6-10-week-old virgin NOD/SCID mice. Four to 6 glands were pooled and digested as described above for tumor organoids, except that digested organoids were centrifuged at 120 x g for 5 min between washes. Tumor and mammary gland explants were imaged 48 h after plating in organotypic culture.

Staining of primary tumor samples. Tissue microarrays containing fixed breast primary tumors (US Biomax) were used for analysis of patient tumors. H&E and immunohistochemical staining was performed as described (Dang, Prechtel et al. 2011). For immunofluorescence analysis, formalin-fixed, paraffin-embedded tissue sections were deparaffinized in xylene and rehydrated in a series of alcohol washes. Antigen retrieval was performed by boiling slides in sodium citrate pH 6.0. Slides were blocked in 20% Aquablock (Abcam, Cambridge, MA) in TBS before being incubated overnight with the indicated antibodies, followed by species-specific secondary antibodies conjugated to AlexaFluor488, AlexaFluor546, or AlexaFluor647, and counterstained with Hoechst.

Supplemental Table 1

Gene.ID	Gene.Name	Fold.Change	q.value...
ILMN_2388800	PPAP2B	17.6675545	0
ILMN_1761425	OLFML2A	14.0026133	0
ILMN_1713499	WISP1	21.7447248	0
ILMN_2408683	PPAP2B	15.1957074	0
ILMN_2246328	PTPN22	10.8650045	0
ILMN_1739496	PRRX1	16.3868209	0
ILMN_1701441	LPAR1	8.7696188	0
ILMN_1776842	DKFZP451A21	10.1198135	0
ILMN_2086470	PDGFRA	37.2154576	0
ILMN_1679267	TGM2	5.56128704	0
ILMN_1702301	DOCK10	4.32890107	0
ILMN_1679060	LOC642559	4.41220235	0
ILMN_3191393	LOC10012889	7.99966671	0
ILMN_1667295	VASN	7.80724662	0
ILMN_1775268	HECW2	4.54521539	0
ILMN_1658917	SLC1A1	5.13386041	0
ILMN_1803423	ARHGEF6	6.35974306	0
ILMN_2213136	LEF1	5.91904804	0
ILMN_1681949	PDGFRA	18.2392571	0
ILMN_1752520	SLFN11	5.6693283	0
ILMN_1715662	CCDC80	5.53603794	0
ILMN_1704418	FOXD1	4.62882767	0
ILMN_1730645	TMEFF2	19.4134978	0
ILMN_1742866	F2R	7.05564733	0
ILMN_2065773	SCG5	27.4926801	0
ILMN_2121408	HBEGF	7.87754231	0
ILMN_1680738	C5ORF13	11.4552373	0
ILMN_1745256	CXXC5	5.94746377	0
ILMN_3232894	CNRIP1	17.224636	1.88665433
ILMN_3307729	CXXC5	5.79209357	1.88665433
ILMN_1709153	PRR16	7.31194642	1.88665433
ILMN_1746618	PAQR7	4.33649065	1.88665433
ILMN_1801516	GPC1	4.79055322	1.88665433
ILMN_1651343	ITGA11	4.57975205	2.7803327
ILMN_2162860	SLFN11	4.90694776	2.7803327
ILMN_1751276	BDNF	10.405662	2.7803327
ILMN_2068499	POU5F1P1	5.00713584	2.7803327
ILMN_1689431	APCDD1L	4.33526196	2.7803327
ILMN_1789394	CATSPER1	5.60085586	2.7803327
ILMN_1712305	CYBRD1	10.0167454	2.7803327
ILMN_1731374	CPE	4.0539856	2.7803327
ILMN_1769556	C5ORF23	4.54380155	2.7803327
ILMN_1676361	ARHGAP22	9.31372039	4.26879364
ILMN_1717934	SYT11	7.44201016	4.26879364
ILMN_2201678	FSTL1	15.6496173	4.26879364
ILMN_1764228	DAB2	5.56233706	4.26879364

ILMN_1801610	METRNL	4.17971401	4.26879364
ILMN_1819854	HS.36053	7.20752808	4.26879364
ILMN_1803338	CCDC80	4.15375642	4.26879364

Supplemental Table 2

GAPDH siGenome pool (CAACGGAUUUGGUCGUAAU, GACCUCAACUACAUGGUU, UGGUUUACAUGUCCAAUA, GUCAACGGAUUUGGUCGUA).

CDC42 siGenome pool (GGAGAACCAUAUACUCUUG, GAUUACGACCGCUGAGUUA, GAUGACCCCUACUAAUUG, CGGAAUAUGUACCGACUGU).

Rac1 SiGenome pool (UAAGGAGAUUGGUGCUGUA, UAAAGACACGAUCGAGAAA, CGGCACCACUGUCCCAACA, AUGAAAGUGUCACGGGUAA).

Non-Targeting OnTargetplus pool (UGGUUUACAUGUCGACUAA, UGGUUUACAUGUUGUGUGA, UGGUUUACAUGUUUUCUGA, UGGUUUACAUGUUUUCUA).

Cdc42 OnTargetplus pool (CGGAAUAUGUACCGACUGU, Cdc42-06: GCAGUCACAGUUAUGAUUG, Cdc42-07: GAUGACCCCUACUAAUUG, Cdc42-08: CUGCAGGGCAAGAGGAUUA).

N-WASP OnTargetplus pool (N-WASP-07: CAGCAGAUCGGAACUGUAU, N-WASP-08: UAGAGAGGGUGCUCAGCUA, N-WASP-09: GGUGUUGCUUGUCUUGUUA, N-WASP-10: CCAGAAAUCACAACAAUA).

DOCK10 OnTargetplus pool (DOCK10-05: GGACCUGACUAAGCGUAUA, DOCK10-06: CAAUAUAGCUACGGAGGUU, DOCK10-07: CAACAUUCGCUUGCAAUUA, DOCK10-08: CCAGACAGCUAUCAAACAU)

DAB2 OnTargetplus pool (DAB2-05: GAACCAGCCUUCACCCUUU, DAB2-06: CAAAGGAUCUGGGUCAACA,
DAB2-07: GAUCUAAACUCUGAAAUCG, DAB2-08: AACUGAAAUCGGGUGUUU)

LPAR1 OnTargetplus pool (LPAR1-06: GAAUGUCUCGGCAUAGUUC, LPAR1-07:
CCACAGUGCUUCUACAACG, LPAR1-08: GCAUGCAGCUCCACACACG, LPAR1-09:
GCACAUGGCUCCUUCGUCA)

ITGA11 OnTargetplus pool (ITGA11-07: UCAAUACAUCGCCAGUGA, ITGA11-08:
GCGAAGAUGUGGUGCAUGA, ITGA11-09: UAAAGGAUUCACACAGUUA, ITGA11-10:
GGACUCAGACGGUAGCAUU)

ARHGEF6 OnTargetplus pool (ARHGEF6-05: GAGGAUGUCUUAUAUCUUA, ARHGEF6-06:
GGACGUUCCUCUUCUUA, ARHGEF6-07: GAGGAGGAAUAUGUGAUUA, ARHGEF6-08:
GGACAUCAUUUACGUCACA)

C5ORF13 OnTargetplus pool (C5ORF13-09: CUUCAGGCCUGGUUCGCUA, C5ORF13-10:
CGGACAUGCAGUCACGGUA, C5ORF13-11: GCACUGCACUUCUUCGUUU, C5ORF13-12:
GAAAGGAUAAUUGUCGAAA)

C5orf23 OnTargetplus pool (C5orf23-09: AGUAAAAGCUGCACACGUU, C5orf23-010:
AGGCAAUUGUGGAAGCGGA, C5orf23-011: GAACAAAGCUGUCACGGUG, C5orf23-012:
AGAUGAAGGCCAUUGCAUA)

CATSPER1 OnTargetplus pool (CATSPER1-06: GCGCGUAUCAUCCAGUUA, CATSPER1-07:
GAAGGGACACUCUACCAAU, CATSPER1-08: ACAAUCCGCUCACGUGUCA, CATSPER1-09:
GCAGAUAGGUUCUUUCGCU)

CCDC80 OnTargetplus pool (CCDC80-17: GGUCAAGAAUGUUGCGUUU, CCDC80-18:
UGAGGAAAGAGUACGGAU, CCDC80-19: CCAUGCUUCUAGUCGAAA, CCDC80-20:
UGGGAGGUCUCGCGGAAU)

CPE OnTargetplus pool (CPE-05: GGAUAGACCACGAUGUUA, CPE-06: GAUGAGACGCGGAGUGGUA,
CPE-07: CCGAGGAGUUAAGGAUUU, CPE-08: AAAGAAGGUGGUCCAAUA)

CXXC5 OnTargetplus pool (CXXC5-09: CCGCAAGAAGAAGCGGAA, CXXC5-10:
GCAUGUUUGUGUCACGAAA, CXXC5-11: GGGCGAAGACAAACGGAUG, CXXC5-12:
GCAGUUGUAGGAAUCGAAA)

CYBRD1 OnTargetplus pool (CYBRD1-09: GGAAGGGAUUAGAUAGCGA, CYBRD1-10:
CAUCAAAGUGUACGGCUU, CYBRD1-11: CAGCUGGGUUGGACUGAUA, CYBRD1-12:
GAACAGGGAGCAAGAGGU)

FOXD1 OnTargetplus pool (FOXD1-05: GUCGAGAACUUUACUGCUA, FOXD1-06:
GCACUGAGAUGUCCGAUGC, FOXD1-07: AAACAGACAUCGACGUGGU, FOXD1-08:
AUAUCGCGCUCAUCACUAU)

FSTL1 OnTargetplus pool (FSTL1-05: GAGAAGAAAUCGUAAGUC, FSTL1-06: GAAACUGCCAUAUAUUA,
FSTL1-07: CCAAAGAGAUCAAUGAGG, FSTL1-08: AGACCGAGGUGGACUGUAA)

LEF1 OnTargetplus pool (LEF1-05: GCAAGAGACAAUUAUGGUA, LEF1-06: UGCCAAAUAUGAAUAACGA,
LEF1-07: CGAUUUAGCUGACAUCAAG, LEF1-08: CGUCACACAUCCCAUCAGA)

METRNL OnTargetplus pool (METRNL-09: GUUAGGAGGCACAGGGCGU, METRNL-10:
AGGAGGUGGAGCAGGUGUA, METRNL-11: GCUGUAAAAUGCAAACUAA, METRNL-12:
CAGAGGAUGUACAGGGAUG)

OLFML2A OnTargetplus pool (OLFML2A-05: GCAGAGAGGCGAGCUGUGA, OLFML2A-06:
GGAUCUAUGUCACCAACUA, OLFML2A-07: AAGCAAGGCCGUGGAGUA, OLFML2A-08:
GCAGUAGAGUCAAGGUUAU)

PPAP2B OnTargetplus pool (PPAP2B-06: GGGACUGUCUCGCGUAUCA, PPAP2B-07:
GGAAUUCUACCGGAUCUAU, PPAP2B-08: GGACAUUAUUGACAGGAAC, PPAP2B-09:
CAUCAAGUACCCACUGAAA)

PPAP2B siGenome pool (PPAP2B-1: GGGACUGUCUCGCGUAUCA, PPAP2B-2:
UCUAUUACCGAAGAAGUC, PPAP2B-3: CAGUUCACCUUGAUGAUGA, PPAP2B-4:
GGAAUUCUACCGGAUCUAU)

PRR16 OnTargetplus pool (PRR16-09: AGGCUAAUGCACCGCUUUAU, PRR16-10:
CGAGUUCGGUUUAAUGAAA, PRR16-11: GCUGCAUACCCAACAGUAA, PRR16-12:
ACGCUGAAUAGUAGCUCAA)

PTPN22 OnTargetplus pool (PTPN22-09: CCUCAGCUGUGAAGGUAAA, PTPN22-10:
GGAGUCAGCUGUACUAGCA, PTPN22-11: GAAUAUAGUGUCCUUAUCA, PTPN22-12:
ACACAGAGGCCUUCAUUAG)

SLFN11 OnTargetplus pool (SLFN11-09: CAGGGAACCUUACGAAUUA, SLFN11-10:
CACCAGGAUAAUUUGCGAUA, SLFN11-11: GGUAUUUCCUGAAGCCGAA, SLFN11-12:
GAGGAGGAGUGAUUCGAAU)

TGM2 OnTargetplus pool (TGM2-05: GCAACCUUCUCAUCGAGUA, TGM2-06:
GCAACGAUGACCAGGGUGU, TGM2-07: GGUCAAUGCCGACGUGGUA, TGM2-08:
GAGACGAGCGGGAGGAUUAU)

TMEFF2 OnTargetplus pool (TMEFF2-09: CCACAUACCUUGUCCGGAA, TMEFF2-10:
CUACAGUGUUCUAUACGUU, TMEFF2-11: UCAAAGAAGCAUCGUGUCA, TMEFF2-12:
GCGACAGGCUGCAUGCAAA)

VASN OnTargetplus pool (VASN-09: UCACAGAACCAGAUCGCCA, VASN-10: ACGAUGAUAUGAAGGCCUU,
VASN-11: ACGCAAAGCCCUACAUCUA, VASN-12: CCAACAGGCUGCAUGAAAU)

WISP1 OnTargetplus pool (WISP1-05: CGCCAGGUCCUAUGGAUUA, WISP1-06:
AACCUGAGCUGUAGGAAUC, WISP1-07: CCAACUAGGCAGGCACAAA, WISP1-08:
ACUCGGAUCUCCAAUGUUA)

PDGFRA MISSION siRNA pool (PDGFRA-01: AACTGATCCCGAGACTCCTG, PDGFRA-02:
GCTGATCCGTGCTAAGGAAG, PDGFRA-03: GCCTATGGATTAAGCCGGTC,)